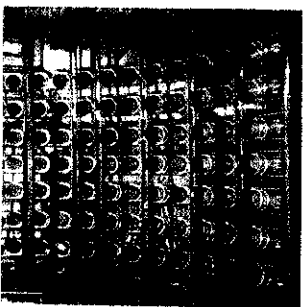
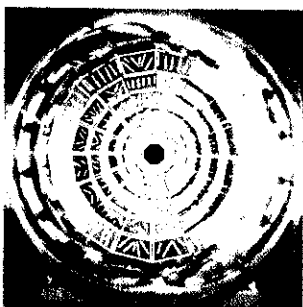
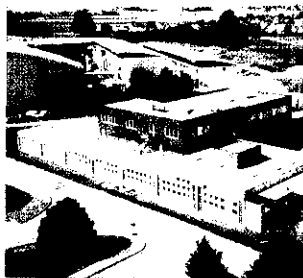


LABORATOIRE DE PHYSIQUE CORPUSCULAIRE



EXPERIMENTS ON SUPER-HEAVY NUCLEI AT GANIL

J. Péter and the Fulis collaboration : N. Alamanos³, N. Amar¹,
J.C. Angélique¹, R. Anne², G. Auger², F. Becker², R. Dayras³, A.
Drouart³, J.M. Fontbonne¹, A. Gillibert³, S. Grévy¹, D. Guerreau², F.
Hanappe¹, R. Hue², A.S. Lalleman², N. Lecesne², T. Legou¹, M.
Lewitowicz², R. Lichtenthäler⁴, E. Liénard¹, W. Mittig², F. De
Oliveira², N. Orr¹, G. Politi⁵, Z. Sosin⁶, M. G. Saint-Laurent², J.C.
Steckmeyer¹, C. Stodel², J. Tillier¹, R. de Turreil², A.C.C. Villari²,
J.P. Wieleczko², A. Wieloch⁶.

1: LPC Caen, France 2: GANIL Caen, France 3: DAPNIA/SPHN, C.E.N.Saclay, France
4: I.F.U.S.P Sao Paulo, Brazil 5: Univ.di Catania, Italy 6: Ins.Fyziki Uniw., Krakow, Poland

LPCC 01-10

Invited paper at International Conference « Nuclear Physics
at Border Lines »

Lipari (Italy), May 21-24 2001

CENTRE NATIONAL DE LA RECHERCHE SCIENTIFIQUE

INSTITUT NATIONAL
DE PHYSIQUE NUCLÉAIRE ET DE PHYSIQUE DES PARTICULES

INSTITUT DES SCIENCES DE LA MATIÈRE ET DU RAYONNEMENT

UNIVERSITÉ DE CAEN

- U.M.R.6534 -

ISMRA - 6. Boulevard Maréchal Juin - 14050 CAEN CEDEX - FRANCE

Téléphone : 02 31 45 25 00 - Télécopie : 02 31 45 25 49

Internet : <http://caeinfo.in2p3.fr>

CERN LIBRARIES, GENEVA



CN-P00038468

EXPERIMENTS ON SUPER-HEAVY NUCLEI AT GANIL

J. PÉTER¹ AND THE FULIS COLLABORATION: N. ALAMANOS³, N. AMAR¹, J.C. ANGÉLIQUE¹, R. ANNE², G. AUGER², F. BECKER², R. DAYRAS³, A. DROUART³, J.M. FONTBONNE¹, A. GILLIBERT³, S. GRÉVY¹, D. GUERREAU², F. HANAPPE¹, R. HUE², A.S. LALLEMAN², N. LECESNE², T. LEGOU¹, M. LEWITOWICZ², R. LICHTENTHÄLER⁴, E. LIÉNARD¹, W. MITTIG², F. DE OLIVEIRA², N. ORR¹, G. POLITI⁵, Z. SOSIN⁶, M.G. SAINT-LAURENT², J.C. STECKMEYER¹, C. STODEL², J. TILLIER¹, R. DE TOURREIL², A.C.C. VILLARI², J.P. WIELECZKO², A. WIELOCH⁶

1 : LPC Caen, France, 2 : GANIL, Caen France, 3 : DAPNIA/SPhN, C.E.N. Saclay, France 4 : I.F.U.S.P., São Paulo, Brazil 5 : Univ. di Catania, Italy 6 : Ins. Fyziki Uniw., Krakow, Poland

1 Introduction

GANIL has several assets which lead us to start a programme on the study of super-heavy nuclei. First, a high beam intensity. Since the cross sections are very low, it is necessary to use beam intensities as large as can stand the target, at least in the microAmpere-particle range ($6.27 \cdot 10^{12}$ projectiles/s), which are produced by ECR sources. Second, a powerful velocity filter: the Wien filter LISE3.

The experimental set-up is described and the performances reached on known isotopes are given in the second and third parts. Short and long range plans for future experiments are described in the following parts: use of $^{76}\text{Ge}_{32}$ beams and, mostly, use of Pb beams to benefit from the assets of inverse kinematics.

2 Experimental set-up.

A complete set-up has been built and tested (see figure). The main tool is the Wien filter with crossed magnetic and electric fields. It is divided into two identical halves and followed by a dipole magnet. It had been designed for the purification of exotic secondary beams produced by fragmentation in the LISE magnetic device and several modifications were found to be necessary for the study of complete fusion evaporation residues (ER's) and the rejection of the primary beam : - a reaction chamber was added just before LISE3, - the upper plate in the first half of the filter was moved up, the beam is thus deflected after this first half without hitting the plate and stopped on a water-cooled plate - two pairs of independently movable slits

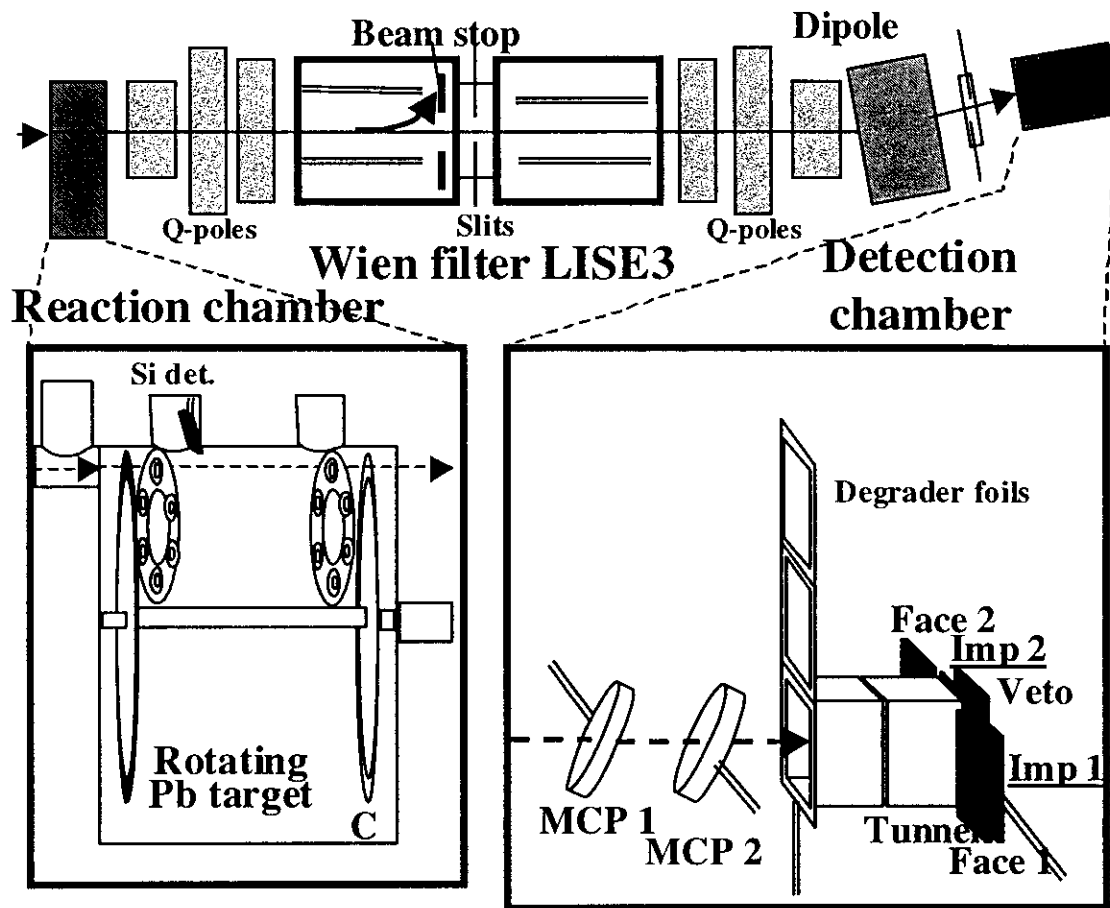


Figure 1 –Experimental set-up

and a beam profiler were installed at mid-filter. The suppression of unwanted products is improved by a dipole magnet located after the velocity filter.

The reaction chamber contains a wheel bearing 35 targets on a diameter of 670 mm and rotating at 2000 RPM, allowing targets with a low melting temperature (Pb, Bi) to sustain intense beams ($1 \text{ particle } \mu\text{A} = 6.25 \cdot 10^{12} \text{ particles/s}$, or more). The time structure of the beam is synchronised with the rotation. A Si detector continuously monitors the status of each target. Smaller rotating targets are used for targets having a higher melting temperature.

The velocity of each product is obtained with 2 aluminized mylar foils and micro-channel plate detectors; its kinetic energy and localisation are given by a X-Y Si implantation detector (Imp). The energy of α -particles and fission fragments escaping from Imp is measured with a "tunnel" of 8 Si detectors. A Si veto detector is installed behind Imp to reject light particles which might punch through it. When emission of α -particles or fission fragment in the Imp is identified via electronics,

the beam is immediately stopped for a short while, during which Imp1 is moved out and Imp2 comes in; then the beam is sent again. α -particles escaping from Imp1 are then detected by the Si detector Face1. It is thus possible to study α -emission or spontaneous fission on long durations without any background. Specific electronics and data acquisition systems were developed. A fast analysis program allows us to identify α -decay chains or spontaneous fission on line.

The transmission of fusion nuclei from the target position through the quadrupoles, filter and final dipole was studied via a simulation code. The optics was checked and the Wien filter was calibrated using low energy (0.35 MeV/u) ions. The response of the whole set-up was checked via fusion reactions with known cross sections and α decay chains: $^{204-206}\text{Fr}$ nuclei formed via $^{86}\text{Kr} + ^{\text{nat}}\text{Sb}$ fusion reactions with cross sections of 10 to 300 μb [Sah85], $^{260,261}\text{Sg}_{106}$ nuclei formed via $^{54}\text{Cr} + ^{208}\text{Pb}$ with cross sections of 300-500 pb [HofMün].

3 Experiments.

3.1 Studies with $^{260,261}\text{Sg}_{106}$

With the ^{208}Pb targets and a ^{54}Cr beam of 40nAp, the silicon implantation detectors measured a counting rate of 5-10 Hz. 2 different energies were used : 4.698 and 4.756 MeV/u. The excitation energies correspond mostly to the 1 neutron evaporation channel ($^{261}\text{Sg}_{105}$, cross section peaking at 500 pb) and to the tail of the 2 n excitation function [HofMün].

With the on-line analysis, we indeed observed 2 decay chains of ^{261}Sg at 4.698 MeV/u whereas at 4.756 MeV/u we observed 9 chains with the characteristics (lifetimes and α energies) attributed to ^{261}Sg and one attributed to ^{260}Sg . The decay chains were identified by position correlation in the Si detector between the implantation of the evaporation residue and the decay by α emission or fission. A transmission efficiency above 60 % and a suppression factor of the primary beam of $2 \cdot 10^{10}$ were achieved.

3.2 Search for element 118.

In 1999 ^{86}Kr on ^{208}Pb studied at Berkeley produced 3 events with a chain of 6 α 's which were attributed to element 118 and its descendants, with a cross section ~ 2.2 pb [Nin99]. The same system studied with the velocity filter SHIP in Darmstadt did not lead to the observation of any event attributable to element 118, with an upper limit of 1 pb [Hof99]. Since Ganil is able to deliver a high intensity beam of ^{86}Kr (15 μA with charge 10+ from CSS1, i.e. nearly 10^{13} projectiles/s) it was decided to try to obtain additional information: i) possible α decay before the minimum time of 120 μs in the Berkeley experiment. This required a faster

acquisition system. ii) detection of α emitted more than 1 mn after implantation of the ER: the movable implantation detector described in the previous section was installed. iii) ER's may be created in an isomeric state which decays via electron capture followed by an electron cascade with an unknown half-life, modifying the ionic charge and strongly reducing the transmission. The carbon stripper foil which re-establishes the ionic charge distribution was located 3 times further, i.e. at larger times, than in the SHIP experiment.

With a total dose of 1.1×10^{18} ions at 5.27 MeV/u no event attributable to a super-heavy nucleus was observed. A similar result was obtained also at RIKEN [Mor00].

4 Plans with $^{76}\text{Ge}_{32}$ Beams.

Cold fusion reactions were used to produce elements 102 to 112 with ^{208}Pb or ^{209}Bi targets and the heaviest isotopes of projectiles ranging from ^{48}Ca to ^{70}Zn [HofMün]. ^{76}Ge projectiles fusing with the heaviest isotopes of targets ranging from Os_{76} to Tl_{81} offer the advantage of forming compound nuclei ranging from $Z=108$ to 113 heavier by 2 neutrons than the compound nuclei formed with ^{208}Pb or ^{209}Bi (except for 111). A similar possibility is offered by $^{82}\text{Se}_{34}$ projectiles [Sto00]. A practical advantage is that only one beam development is needed.

The difficult point is to estimate which cross sections will be obtained. Compared to $^{208}\text{Pb} - ^{209}\text{Bi}$ induced reactions, the entrance channel is more symmetric and there is no closed shell in the partners. Both points are known to reduce the fusion cross section. An estimate of the reduction factors can be made using the ER cross sections observed for the compound nucleus ^{220}Th formed via different entrance channels having similar Bass barriers, as shown in figure 2 [Sah84, Sah85, Ver84, Sto98]. At the same excitation energy, 45 MeV, the effect of the deexcitation step is expected to be the same and the difference in the xn cross sections is attributed to entrance channel characteristics.

$\text{Ar}_{18} + \text{Hf}_{72}$ and $\text{Zn}_{30} + \text{Nd}_{60}$ systems have no closed shell in any partner. Even though it has a smaller Bass barrier, the more symmetric system $\text{Zn} + \text{Nd}$ has a cross section smaller by a factor 14 than $\text{Ar} + \text{Hf}$. Assuming a steady variation of the cross section with the charge asymmetry, the expected cross sections for $\text{Ca}_{20} + \text{Yt}_{70}$ and $\text{Zr}_{40} + \text{Sn}_{50}$ are estimated. The actual cross sections are much higher, by factors 6 and 23 respectively, due to the role of the closed shells [Mol97]: 20n and 28p in $^{48}\text{Ca}_{20}$, 50p in Sn_{50} .

These factors may now be used to estimate the reduction factor which apply when the same compound nucleus (and ER) is formed via $^{76}\text{Ge} + \dots$ instead of $^{208}\text{Pb} - ^{209}\text{Bi} + \dots$ since the excitation energies at the Bass barrier are very close. The loss of shell effects is estimated to reduce the cross section by an order of magnitude. At

Z=106 the decrease of charge (and mass) asymmetry reduces the cross section by a factor about 12. This asymmetry disappears for $^{76}\text{Ge}+^{208}\text{Pb}$ reactions (element 114).

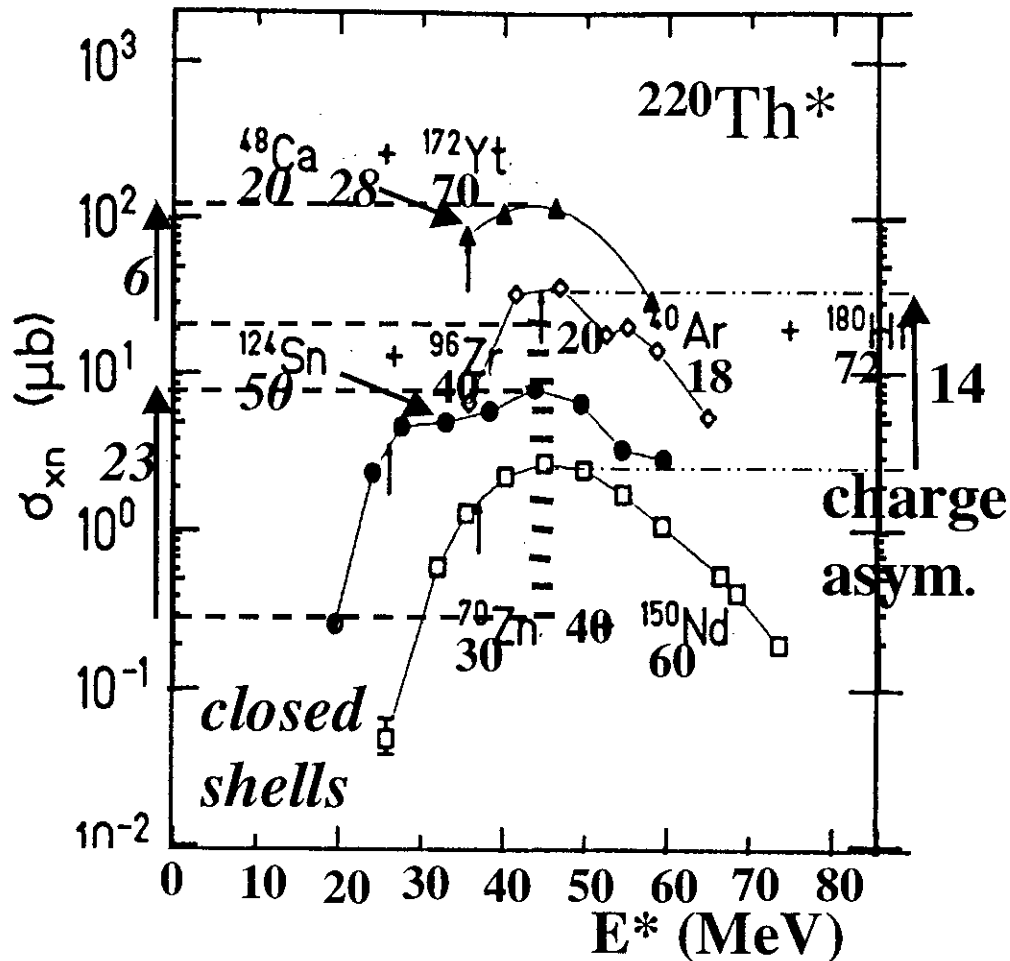
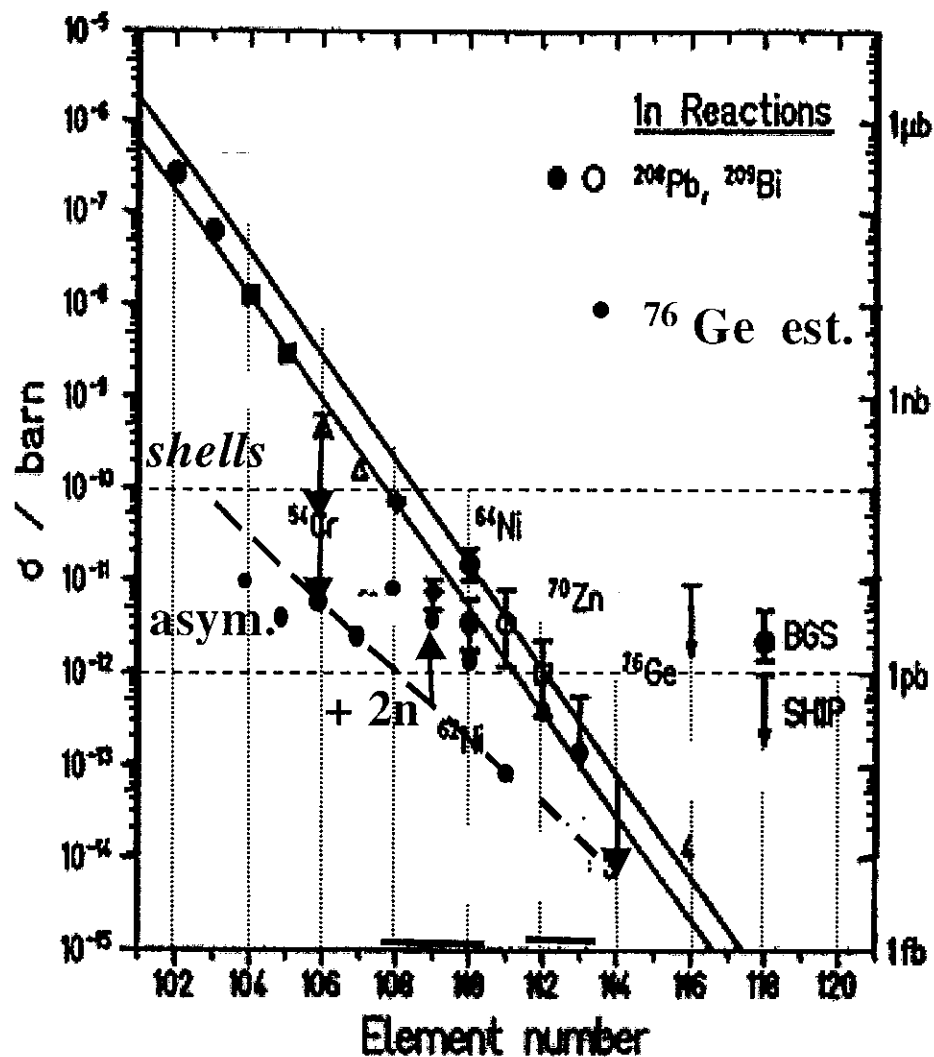


Figure 2 – Excitation functions of evaporation residues (xn) of ^{220}Th compound nuclei formed via different entrance channels [Sah84,Sah85,Ver84,Sto98].

Therefore, the dashed line in figure 3 represents the cross sections which would be obtained for Ge induced reactions leading to the same 1n ER's as $^{208}\text{Pb}-^{209}\text{Bi}$ induced reactions. For Z=106, 107 and 111, this is the case. For Z=108,109,110,112,113, compound nuclei may be formed with 2 additional neutrons. Detailed measurements made for Th isotopes show that 2 more neutrons in the compound nucleus increase the residue cross section by a factor 9 [Sto98]. As seen in fig. 3, for Z=110 the use of ^{64}Ni instead of ^{62}Ni on ^{208}Pb results in an increase by a factor ~5. An average factor 7 is used in figure 3.

The cross sections thus estimated are smaller than ^{208}Pb - ^{209}Bi induced reactions. ^{84}Se induced reactions make more symmetric entrance channels and therefore smaller cross sections. Of course these empirical estimates are subject to large uncertainties: the reduction factors may be larger or smaller, the role of target deformation is not taken into account... Theoretical predictions were asked to authors who reproduced the cross sections of ^{208}Pb and ^{209}Bi induced reactions: [Ada98, Den00, Gia00, Ari00 and Oht00]. These calculations are also subject to large uncertainties (role of deformation, unknown values of fission barriers,...), but

Figure 3 : \ln cross sections measured for ^{208}Pb and ^{209}Bi induced fusion [Hof99] and estimated for ^{76}Ge induced fusion: see text



they confirm that ^{82}Se projectile is less favorable than ^{76}Ge and that, even with ^{76}Ge , the cross sections are expected to be well below those of ^{208}Pb - ^{209}Bi induced reactions [private communications].

A specific interest of these reactions [Sto00] is the direct cold fusion production of $^{273}110$ ($^{76}\text{Ge} + ^{198}\text{Pt} = ^{273}110 + 1n$) in order to establish the production of element 112. Indeed different α -decay energies and lifetimes had been observed for the few events of $^{273}110$ produced in the decay of $^{277}112$ obtained via cold fusion ($^{70}\text{Zn} + ^{208}\text{Pb}$) [HofMun.] and in direct hot fusion production of this isotope: $^{34}\text{S} + ^{244}\text{Pu} = ^{273}110 + 5n$ [Laz95]. At this conference, S. Hofmann showed that the decay chains of $^{277}112$ are now understood. The α spectroscopy of $^{273}110$ is of interest since the population of these different levels (especially isomeric states) may be due to overreaching the deformed shell $N=162$, but it would require a "large" number of events, which would need a very long beam time with cross sections in the pb range.

5 Assets of inverse kinematics.

The use of inverse kinematics has an obvious drawback: the velocity difference between the beam and the evaporation residues is much smaller and larger magnetic and electric fields are necessary in a velocity filter. LISE3 is powerful enough to obtain the same separation at mid-filter (fig. 1). Another difficulty is the larger energy deposit in the target and the stripper foil. The targets have higher melting temperatures than Pb or Bi., but mechanical effects (micro-holes) are more important.

There are however several assets relative to usual kinematics. The first gains concern the beam time:

- the target thickness is no longer limited by multiple scattering of the ER's in the target. Therefore, instead of covering only 3-4 MeV in excitation energy, a target thick enough to cover the whole excitation function of interest may be used: 8 to 12 MeV, thereby maximising the counting rate. The most important application is the search for an unknown isotope. Indeed different mass defects in different mass tables lead to incident energies differing by several MeV whereas the excitation function is rather narrow (a few MeV). In usual kinematics, lengthy measurements at several incident energies must be made, but only one in inverse kinematics.

- the strong forward focussing of ER's ensures a better transmission, even after α -decay in flight.

- the ionic charge distribution of ER's is better estimated and its relative width is smaller, improving the transmission..

The other gains concern the quality of the data:

- the energy deposited by an implanted ER is large and measured with a much better accuracy so that it is able to provide, combined with the time-of-flight, an estimate of the mass. This is valuable additional information
- due to the deeper penetration of ER's in the implantation detector, both spontaneous fission fragments are stopped in this detector and the fission total kinetic energy is easily measured. α -particles emitted backwards leave at least 2 MeV in this detector and cannot be missed.

6 : Plans with Pb beams.

This method is suitable for several aspects of super-heavy nuclei studies and can be applied to all systems. We will first use it to the reactions which were found to have the largest cross sections up to $Z=112$: cold fusion of ^{208}Pb with neutron-rich isotopes [HofMün]. In order to get new information on super-heavy nuclei, several systems, listed in the table below, can be studied for different purposes:

	Z	208Pb +...			207Pb +...		
		Tget	ACN	E*Bass	Tget	ACN	E*Bass
Rf	104	50Ti	258	23	50Ti	257	23
Db	105		259	25	51V	258	25
Sg	106	54Cr	262	22	54Cr	261	22
Bh	107		263	24	55Mn	262	24
Hs	108	58Fe	266	21	58Fe	265	20
Mt	109		267	23	59Co	266	22
	110	64Ni	272	17	64Ni	271	16
	111		273	19	65Cu	272	18
	112	70Zn	278	12	70Zn	277	12
	113	71Ga	279	13	71Ga	278	13
	114	76Ge	284	9	76Ge	283	9
	115	75As	283	13	75As	282	13
	116	82Se	290	3	82Se	289	2
	117	81Br	289	7	81Br	288	6

bold letters: new reactions

new isostopes

new isostopes

1 - **New paths to known isotopes with ^{208}Pb .** The same compound nuclei and ER's with odd Z formed at GSI with a ^{209}Bi target and an even Z projectile can be formed with a ^{208}Pb beam and a target with an odd Z. Two points are of interest: 1- to measure the cross section and to compare it to the known cross section with ^{209}Bi . That will give a clue to the respective roles of macroscopic and structure effects on the ER cross section: charge asymmetry of the entrance channel and closed shells in the partners. Indeed fusion with ^{208}Pb is less favoured due to the larger Coulomb repulsion and excitation energy at the interaction barrier, but this may be partially compensated by its exactly filled shells. 2- to reach different levels in the ER, especially isomeric states indicated by an unusually large value of alpha-particle energy.

2 - **Studies of Spontaneous Fission and α energies.** For elements ranging from Fm_{100} to Rf_{104} the mass distributions are known to vary rapidly from symmetric to asymmetric shapes as a function of Z and A of the fissioning nucleus. The total kinetic energy (TKE) distributions also exhibit different shapes [DHof95] and can be measured. In direct kinematics most events leave a part of their energy in the entrance windows of the implantation detector and one of the tunnel detectors, and the TKE of each event is affected by a different loss. As noted above, in inverse kinematics the whole TKE is measured in the implantation detector. Such studies will be made first on nuclei with a large spontaneous fission probability and cross sections in the hundreds of pb range: $^{260}\text{Sg}_{106}$ (about 50 % of s. f.) and its α decay product $^{256}\text{Rf}_{104}$.

3 - **New isotopes with ^{207}Pb .** Isotopes lighter by 1 neutron than the known isotopes of several elements can be produced with ^{207}Pb instead of ^{208}Pb : with ^{55}Mn the 2n channel leads to $^{260}\text{Bh}_{107}$ - ^{59}Co , 1n : $^{265}\text{Mt}_{109}$ - ^{65}Cu , 1n : $^{271}\text{111}$ - ^{70}Zn , 1n : $^{276}\text{112}$. For these last two cases, a chain of 3 α 's will be observed before reaching a known isotope, i.e. 3 new isotopes will be observed in one event.

$^{276}\text{112}$ offers the special interest of being an even-even nucleus. Its α decay and spontaneous fission are unhindered and can be more easily compared with theoretical predictions than nuclei with unpaired nucleon(s). In addition its level scheme is expected to be simpler

4 - **New elements.** Above $Z=109$, the counting rate is very low. For $^{277}\text{112}$ measurements were made at one beam energy only, which is not necessarily at the maximum of the excitation function. Indeed the 1n excitation function seems to have its maximum shifted to smaller values with Z (due to the decrease in the fission barrier height) and also to become narrower [HofMün]. The broad energy coverage provided by inverse kinematics may reveal a larger cross section value.

The 1n channel cross section decreases quickly with Z. It may be that the 0n cross section (radiative capture, i.e. compound nuclei formed at excitation energies smaller than the neutron separation energy S_n , 7-8 MeV) becomes larger than the 1n

cross section, even though the fusion probability drops very much at the corresponding incident energy. Added to the uncertainty on the compound nucleus mass defect, the exploration of the broad range of incident energies corresponding to $0n + 1n$ excitation functions leads to lengthy measurements at several incident energies in direct kinematics : 6 beam energies were tried for Se+Pb in a search for element 116 [HofMün]. With a Pb beam, an excitation energy range of 12 MeV or more can be covered with a single incident energy.

7 References

- Ada98: G. G. Adamian et al., Nuc. Phys A 633, 409 (1998)
Ari00: Y. Aritomo et al., Proc. Int. Workshop Fusion, Dubna, May 2000, World Sci.
Den00 : V. Yu. Denisov and S. Hofmann, Phys. Rev. C 61,034606 (2000)
Dhof95 : D.C. Hoffman and M. R. Lane, Rad. Acta **70/71**, 135 (1995).
Gia00: G. Giardina et al., Eur. Phys. J. A 8, 205 (2000)
Hof99 : S. Hofmann, Proc. Int. Conf. Sevilla (1999)
HofMün : S. Hofmann, G. Münzenberg Rev. Mod. Phys. 2000)
Möl97 : P. Möller et al, Z. Phys. A 359, 251 (1997)
Nin99 : V. Ninov et al., Phys. Rev. Lett. **83**, 104 (1999)
Oht00 : M. Ohta, Proc. Int. Workshop Fusion, Dubna, May 2000, World Sci.
Dhof95 : D.C. Hoffman and M. R. Lane, Rad. Acta **70/71**, 135 (1995)
Mor00: K. Morita, comm. at Int. Workshop Fusion, Dubna, May 2000
Mor91 : W. Morawek et al. Z. Phys. **A341** (1991) 75 and report GSI-91-26
Sah85 : C.C. Sahm et al., Nuc. Phys. A441,316 (1985)
Sto98 : C. Stodel, PhD thesis, LPC Caen (1998)
Sto00 : C. Stodel et al., Tours Symposium on Nuclear Physics, September 2000